

Serveur Académique Lausannois SERVAL serval.unil.ch

Author Manuscript

Faculty of Biology and Medicine Publication

This paper has been peer-reviewed but does not include the final publisher proof-corrections or journal pagination.

Published in final edited form as:

Title: Gene transfer engineering for astrocyte-specific silencing in the CNS.

Authors: Merienne N, Delzor A, Viret A, Dufour N, Rey M, Hantraye P, Déglon N

Journal: Gene therapy

Year: 2015 Oct

Volume: 22

Issue: 10

Pages: 830-9

DOI: [10.1038/gt.2015.54](https://doi.org/10.1038/gt.2015.54)

In the absence of a copyright statement, users should assume that standard copyright protection applies, unless the article contains an explicit statement to the contrary. In case of doubt, contact the journal publisher to verify the copyright status of an article.

Gene transfer engineering for astrocyte-specific silencing in the CNS

Merienne Nicolas, MSc ^{1,2,5}, Delzor Aurélie, PhD ^{3,4,5}, Viret Amaya, MSc ^{1,2}, Dufour
Noëlle, MSc ^{3,4}, Rey Maria ^{1,2}, Hantraye Philippe, PhD ^{3,4} and Déglon Nicole, Pr ^{1,2*}

¹Laboratory of Cellular and Molecular Neurotherapies (LCMN), Department of Clinical Neurosciences, Lausanne University Hospital, Lausanne, Switzerland; ²LCMN, Neuroscience Research Center (CRN), Lausanne University Hospital, Lausanne, Switzerland, ³Commissariat à l'Energie Atomique et aux Energies Alternatives (CEA), Institute of Biomedical Imaging (I2BM), Molecular Imaging Research Center (MIRGen), Fontenay-aux-Roses, France; ⁴CNRS-CEA URA2210, Fontenay-aux-Roses, France; ⁵These authors equally contributed to these work.

Running title: Cell-type specific gene silencing in the CNS

*Correspondence should be addressed to N.D. (nicole.deglon@chuv.ch)

Nicole Déglon
Lausanne University Hospital (CHUV)
Pavillon 3, Avenue de Beaumont
1011 Lausanne
Switzerland
Phone: +41 21 314 21 20
Fax: +41 21 314 08 24

Number of words: 7023 (including figures)

ABSTRACT

Cell-type specific gene silencing is critical to understand cell functions in normal and pathological conditions, in particular in the brain where strong cellular heterogeneity exists. Molecular engineering of lentiviral vectors (LV) has been widely used to express genes of interest specifically in neurons or astrocytes. However, we show that these strategies are not suitable for astrocyte-specific gene silencing due to the processing of shRNA in a cell. Here, we develop an indirect method based on a tetracycline-regulated (Tet) system to fully restrict shRNA expression to astrocytes. The combination of Mokola-G envelope pseudotyping, glutamine synthetase (GS) promoter and two distinct miRNA target sequences provides a powerful tool for efficient and cell-type specific gene silencing in the CNS. We anticipate our vector will be a potent and versatile system to improve the targeting of cell populations for fundamental as well as therapeutic applications.

INTRODUCTION

Cell-type specific overexpression or silencing of a gene of interest has been used to dissect cellular functions and to assess the therapeutic benefits of gene therapy. *In vivo*, this has been investigated in transgenic animals or following the intracerebral injection of viral vectors, and may involve tissue-specific promoters to control transgene expression^{1,2}. The injection of viral vectors provides an efficient gene transfer system irrespective of the species considered, age of the animals and the targeted organ³. Moreover, viral vectors are simple to produce⁴. Among them, lentiviral vectors (LV) have a large cloning capacity, high transduction efficiency and can be engineered to restrict transgene expression to particular cell subtypes^{5,6}. The pseudotyping of LV particles with the glycoprotein G of the vesicular stomatitis virus (VSV-G) results in efficient neuronal targeting with ubiquitous promoters⁷ whereas both neurons and astrocytes are transduced when LV is pseudotyped with the glycoprotein G of the Mokola virus (MOK-G)⁸. Tissue-specific promoters may be used to restrict further transgene expression to a particular cell subpopulation. However, these transcriptional regulatory elements are still poorly characterized and there are few examples of tightly regulated transgene expression involving viral vectors^{9,10}. Regulation involving miRNA has been explored as an alternative strategy¹¹. For CNS applications, we demonstrated that four copies of the neuron-specific miRNA-124 target sequence (miR124T) in a Mokola-pseudotyped LV (MOK/LV) specifically suppresses transgene expression in neurons and not in astrocytes¹². We also showed that this vector efficiently silences the GLAST gene, expressed mainly in astrocytes¹². However, during small-hairpin RNA (shRNA) processing and maturation, miRT sequences should be cleaved from the mature shRNA; therefore, we hypothesized that this vector would not be suitable to induce glial-specific loss-of-function phenotypes of ubiquitously expressed genes. We sought to overcome this issue to investigate further the physiological functions and contribution of glial cells to neurodegenerative diseases. Therefore, we indirectly regulated the expression of shRNA with a tetracycline-regulated (Tet) system in a single MOK/LV. The combination of this Tet-regulated system with a tissue-specific promoter and miRNA regulation leads to the

robust silencing of gene expression in glial cells. This approach may be potentially extended to other cell populations for which cell-type specific promoters and miRT are available and provides a powerful system to restrict transgene expression in distinct cell populations.

RESULTS

A miRNA detargeting approach is not suitable for LV constitutively expressing shRNA

We hypothesized that a classical detargeting approach is not appropriate for a cell-type specific gene silencing due to the processing of the shRNA (Fig. 1C). This was confirmed by injecting a VSV-G pseudotyped LV expressing a miR30-embedded shRNA targeting the GFP (shGFP) under the control of the phosphoglycerate kinase 1 (PGK) promoter with 4 copies of the fully homologous miR124T sequence (PGK-miR30-shGFP-miR124T, hereafter called VSV/LV-shGFP-miR124T) into the striatum of BAC-Drd2-eGFP transgenic mice expressing the enhanced green fluorescent protein (GFP) in striatal neurons of the indirect pathway^{1,7,13}. As a negative control, we used an LV expressing an shRNA showing no homology with the mouse transcriptome (VSV/LV-shUNIV) and as a positive control, we used a LV expressing the shGFP without miR124T sequences (VSV/LV-shGFP). We also co-injected a VSV/LV expressing DsRed under the PGK promoter to visualize the injection site and facilitate post-mortem analysis (VSV/LV-DsRed; Fig. 1A). Pictures of the infected areas show the extensive loss of GFP expression in animals injected with the positive control expressing the shGFP in neurons (VSV/LV-shGFP), whereas this is not observed in the shUNIV group (Fig. 1A-B). DsRed fluorescence in the GFP-negative area confirms that the silencing is not due to toxicity or cell death induced by LV injection. GFP expression was significantly impaired in animals that received the VSV/LV-shGFP-miR124T. Quantification of the volume of GFP silencing shows that there is no statistical difference between VSV/LV-shGFP-miR124T and VSV/LV-shGFP groups (Fig. 1B). This shows that despite the presence of the miR124T sequences on the vector, GFP silencing is occurring in neurons. Thus, these results demonstrate that a direct coupling of the miRT sequence to the miRNA-embedded shRNA is not suitable for astrocyte-type specific gene silencing, probably due to the cleavage of miRT sequences from shRNA during miRNA processing (Fig. 1C).

Development of an alternative strategy: a tetracycline-regulated (Tet) system

In order to circumvent this limitation, we indirectly controlled the tissue-specific expression of shRNA with the tetracycline-regulated transactivator (tTA/S2). In this system, shRNA expression is driven from a Tet-responsive element (TRE) fused with the minimal cytomegalovirus promoter (CMVmin), and the tTA/S2 is under the control of a polymerase II promoter and miR124T sequences (Fig. 1D). When the LV transduces neurons, the endogenous miR124 recognizes the miR124T present at the 3' UTR of the tTA/S2 and induces the degradation of the tTA/S2 mRNA. Thus, the shRNA is not expressed in neurons. In contrast, when the LV infects astrocytes, the tTA/S2 is expressed and binds to the TRE to induce shRNA expression.

Effect of astrocytic promoters on LV tropism

We tested different astrocytic promoters as a first step towards the establishment of an astrocyte-specific silencing system. We injected MOK/LV expressing the nuclear DsRed (DsRednuc) under the control of the human excitatory amino acid transporter 1 (EAAT1), the human glial fibrillary acidic protein (gfaABC₁D), or the rat glutamine synthetase (GS) promoter into the striatum of adult BAC-GLT1-eGFP transgenic mice expressing GFP in astrocytes¹⁴. As a control, we used a MOK/LV expressing DsRednuc under the ubiquitous cytomegalovirus (CMV_α) promoter. We used the neuronal marker NeuN and GFP-positive astrocytes to determine the tropism of the vectors (Fig. 2A). All promoters, including the CMV_α promoter, gave rise to strong astrocytic expression of the transgene, with at least 88% of the DsRednuc-positive cells co-localized with GFP and NeuN/DsRednuc double-stained cells were scarce (Fig. 2B).

Combined effects of an astrocytic promoter and miR124T detargeting on LV tropism

We sought to improve further the tissue-specificity and eliminate residual transgene expression in neurons (up to 12%); therefore, we added four copies of the miR124T sequence to the 3' UTR of the DsRednuc reporter gene. We pseudotyped the CMV_α, EAAT1, gfaABC₁D and GS-DsRednuc-miR124T LVs with MOK-G and injected them into the

striatum of GLT1-eGFP mice. The animals were killed three weeks later and sections were processed for NeuN immunostaining. Quantitative analysis of the co-localization between DsRednuc and either GFP or NeuN staining revealed that the miR124T sequence improved the specificity of vector containing the GS promoter, whereas the tropism was not modified in the other conditions (Fig. 2C-D). In particular, GS and *gfaABC₁D* promoters lead to more than 95% of astrocyte-specificity and could thus be of interest for the design of astrocyte-specific vectors. Qualitative observations during image acquisition indicate that the GS promoter is more efficient, in agreement with the expression profile of *gfap* (coding for GFAP protein) and *glul* (coding for GS protein) genes from the Allen Brain Atlas microarray data (<http://www.brain-map.org>)¹⁵ (Supplementary Fig. 1). Thus, considering the astrocytic tropism and level of expression, we chose the GS promoter to pursue the study.

Functionality and tropism of the Tet-regulated LV

To establish the functionality and tropism of the Tet-regulated system with cell-type specific promoters and detargeting strategy, we integrated the GS and the miR124T into a single tetracycline-regulated lentiviral backbone pseudotyped with the MOK-G envelope¹⁶ expressing a nuclear GFP cassette (AcGFPnuc) (Supplementary Fig. 2A). In BAC-GLAST-DsRed transgenic mice expressing the DsRed gene specifically in astrocytes¹⁴, the reporter gene was expressed in astrocytes, with $75.2 \pm 3.5\%$ of AcGFPnuc-positive cells co-localized with astrocytic markers with the GS-miR124T vector (Supplementary Fig. 2B). This shows that, despite a lower astrocytic tropism than constitutive vectors (Figure 2), the Tet-regulated backbone is functional in the mouse striatum and provides an appropriate vector for further development.

Efficiency and specificity of the Tet-regulated LV-shRNA

Figure 2 and Supplementary Figure 2 demonstrate that transgene overexpression under the GS promoter without miR124T sequences or in the Tet-regulated system leads to a strong astrocytic tropism. To demonstrate the added value of a Tet-regulated system for cell-type specific gene silencing, we integrated a miR30-embedded shGFP in constitutive and Tet-

regulated backbones (MOK/LV-Tet-shGFP-miR124T, Tet-shGFP; MOK/LV-GS-shGFP, GS-shGFP) (Fig. 3A). We co-injected these vectors with a VSV/LV-DsRed into GLT1-eGFP mice and examined brain sections 3 weeks post-transduction to determine the efficiency of silencing. Mosaic acquisitions indicate that the silenced area is equivalent between inducible and constitutive systems (Fig. 3B). However, the mean fluorescence intensity in the silenced area with the constitutive system is higher than with the Tet-regulated construct, demonstrating that silencing with the Tet-regulated system is more potent (Fig. 3C). This shows that, despite a strong astrocytic tropism for both vectors, shGFP expression in a Tet-regulated backbone provides a more powerful silencing efficiency, which is probably due to the amplification loop of the system leading to greater transgene expression and confirm the important added value of the Tet system¹⁶.

To quantify the specificity of the Tet-regulated system, and in particular potential residual silencing activity in neurons, we used a bicistronic LV coexpressing mCherry and GFP in neurons¹⁷ (VSV-G/LV-mCherry-GFP) (Fig. 3D). We measured GFP and mCherry fluorescence intensity in individual neurons and determined a GFP/mCherry ratio: if residual GFP silencing occurs in neurons, the ratio will be low. We co-injected the MOK/LV-Tet-shGFP-miR124T (Tet-shGFP-miR124T) or MOK/LV-Tet-shUNIV-miR124T (Tet-shUNIV-miR124T) vectors with the neurotropic VSV-G/LV-mCherry-GFP into the striatum of C57Bl/6 mice and analyzed fluorescence intensity 3 weeks post-injection. Pictures were acquired for each channel and the mean fluorescence intensity per cell (MFI/cell) was quantified for both GFP and mCherry. The GFP/mCherry ratio for the negative control (Tet-shUNIV-miR124T) was arbitrarily set at 1. The GFP/mCherry ratio in the Tet-shGFP-miR124T group was significantly lower than that of the Tet-shUNIV-miR124T group, demonstrating a residual GFP silencing in neurons (Fig. 3D). Together with data from Supplementary Fig. 2, these results demonstrate that the transgene expression in Tet-regulated LV is powerful but not tightly restricted to astrocytes and thus needs to be improved.

Combination of miR9*^T-miR124T sequences for efficient and specific silencing in astrocytes

Previous studies have demonstrated the benefit of combining two distinct miRT sequences to suppress transgene expression in a specific cell population¹⁷. These effects depend on miRNA levels and activity, but additional factors influence the extent of suppression¹⁷. We therefore chose a second miRNA, the miR9* to improve the cell-type-specific expression in astrocytes¹⁷ and demonstrated the functionality of the construct in a MOK-G/LV (Supplementary Fig. 3).

We then generated a MOK/LV-Tet-shGFP-miR9*T-miR124T vector (Tet-shGFP-miR9*T-miR124T) and injected it into the striatum of BAC GLT1-eGFP transgenic mice to assess the silencing efficiency (Fig. 4A). As negative control, we used a MOK/LV-Tet-shUNIV-miR9*T-miR124T (Tet-shUNIV-miR9*T-miR124T) vector. We co-injected the vector expressing DsRed into neurons (VSV/LV-DsRed; Fig. 4B) to visualize the infected area to guide quantifications. Brains were collected 3 weeks post-transduction and the efficiency of the GFP silencing was determined by measuring the volume of GFP loss in the striatum. Pictures show extensive GFP loss around the DsRed-positive infected area (Fig. 4B); GFP was silenced in more than 1mm³ of striatum in animals infected with the Tet-shGFP-miR9*T-miR124T construct, whereas GFP was not silenced in the animals that received the Tet-shUNIV-miR9*T-miR124T vector (Fig. 4C). This result demonstrates the silencing efficacy of the Tet system regulated by multiple miRT sequences.

As a final validation of the construct, we assessed the specificity of the vector with the bicistronic VSV/LV-mCherry-GFP system. We used the Tet-shUNIV-miR9*T-miR124T vector as a negative control and an shGFP expressed from the PGK promoter (PGK-shGFP) as a positive control. We co-injected viral vectors into the striatum of C57Bl/6 mice and collected brains 3 weeks post-transduction. The fluorescence intensity of the mCherry was used as a reference to determine the GFP/mCherry ratio in each group (Fig. 4D-E). As expected, the GFP/mCherry ratio was significantly lower with the positive control (PGK-shGFP, neuronal silencing) than with the negative control (Fig. 4D-E). The GFP/mCherry ratio was not statistically different between the Tet-shUNIV-miR9*T-miR124T and the Tet-shGFP-miR9*T-miR124T-infected groups (Fig. 4D-E), whereas a significant difference was observed between shGFP and shUNIV groups containing only the miR124T (Figure 3D). The

difference between these two constructs demonstrates that the combination of multiple miRT sequences with cell-type specific promoters in Tet-regulated system results in a strong astrocyte-specific gene silencing.

DISCUSSION

The advent of whole-transcriptome profiling provides unprecedented opportunity to study gene expression and cellular functions in the brain. However, new experimental systems are required to take into account the diversity of CNS cell-types, unravel the contributions of individual subpopulations and characterize further the diversity of cellular phenotypes in physiological and pathological conditions. The overexpression or silencing of genes are prototypical experimental paradigms to address these questions. Currently, *in vivo* astrocyte-specific loss of function studies rely on the development of knockout mice or take advantage of mice expressing Cre recombinase under the control of cell-type specific promoters to knock-out floxed genes ². Recently, various fragments of the GFAP promoter have been used as transcriptional control elements in viral vectors to restrict transgene expression to astrocytes ^{10, 18}. AAVs have been used for astrocyte-specific gene overexpression. This has involved the use of specific serotypes and astrocytic promoters. However, they have not yet been used for cell-type specific silencing and the small packaging size of AAVs limits the integration of complex and large expression cassettes in astrocytes ^{10, 19}. In addition, the choice of LV envelope could have an impact on the viral vector tropism. We used MOK-G/LV due to their natural preferential tropism for astrocytes ^{12, 20}. If VSV-G/LV have the potential to transduce astrocytes ²¹, the combination of VSV-G/LV envelope, PGK promoter and miR124T was not sufficient to fully restrict transgene expression to astrocytes ¹².

In the present study, we developed a new LV, which enables local, cell-type specific, and tightly controlled silencing *in vivo*. We were able to achieve astrocyte-specific silencing with this vector as a proof-of-principle. We combined a single Tet-regulated lentiviral vector, integrating an indirect miRT detargeting strategy, with Mokola pseudotyping and an astrocytic promoter to control RNAi activity and avoid transgene expression in unwanted cells.

We tested three astrocytic promoters in MOK-G pseudotyped LV. We used a reporter gene to facilitate the characterization of the tropism in the striatum of adult mice. All promoters, including the CMV promoter, resulted in more than 90% of reporter gene expression in astrocytes, with or without the insertion of the miR124T. Similar results have been reported with MOK-G pseudotyped LV expressing GFP and glial cell line-derived neurotrophic factor (GDNF) under the CMV promoter ²⁰. In contrast, in VSV-G pseudotyped LV, the CMV promoter leads to neuronal transgene expression with limited transcriptional activity in astrocytes, suggesting that the choice of the envelope has an impact on the tropism of LV-CMV ^{7, 22}.

Another important factor in the selection of a tissue-specific promoter is its transcriptional activity. Cell-type specific promoters are often associated with weak transgene expression, as demonstrated for the EAAT1 promoter ¹². The GS and GFAP proteins are produced in astrocytes and synthesized to a small extent in neurons ^{23, 24}. Microarray data in the mouse striatum indicate that the GS promoter has a higher transcriptional activity than the GFAP promoter, confirming the utility of this promoter for gene transfer applications ¹⁵. Additional expression profile studies are needed to characterize promoters with a higher transcriptional activity.

When we transferred the system into the single Tet-regulated vector, the residual activity in neurons was significantly higher than in the constitutive vector. This phenomenon has been observed both for reporter gene overexpression and for gene silencing (Supplementary Fig. 2 and Fig. 4). This phenomenon reflects the leakiness of the Tet-regulated system and is coherent with previous studies ^{16, 25}. Indeed, the tetracycline system can lead to residual activity in the “off” stage when two independent vectors are used ^{25, 26}. Incorporation of the entire system into a single LV and modifications of the central polypurine tract (cPPT) and woodchuck hepatitis virus (WHV) elements drastically reduce the basal expression ²⁵. Despite a significant improvement with this combination, residual activity is high when a tissue-specific promoter regulates the expression of the transactivator ²⁵. One additional hypothesis to explain this leakiness is that the tetracycline system creates an amplification

loop which enhances transgene expression^{26, 27}. This is conceivable because GS transcriptional activity in the constitutive system was not associated with detectable transgene expression in neurons, whereas in the inducible system, residual reporter gene expression was detected.

We combined the miR124T sequence with a second miRT to provide additive or synergistic effects to overcome the limitation of residual transgene activity in unwanted cells¹⁷. Brown and collaborators elegantly demonstrated the potency of this strategy when miR target sequences of highly expressed, cell-type specific miRNAs are integrated into the 3' UTR of a gene^{11, 28}. In our study, we selected two miRNAs known to be highly active in neurons; miR124 and miR9*²⁹⁻³¹. The efficiency of miRNA regulation is correlated with the number of target sequences and the restriction of transgene expression to one particular cell type is facilitated by the use of target sequences for two miRNAs; therefore, we used four copies of each fully homologous miR124T and miR9*T to ensure a rapid and efficient detargeting effect³². The insertion of these sequences into the Tet-regulated vector completely blocked residual expression in neurons.

This new LV provides a powerful and flexible system for astrocyte-specific gene silencing in adult animals and is complementary to experimental design based on transgenic mice. In addition, this system can be adapted to generate vectors suitable for silencing in other subpopulations of cells in the brain or peripheral organs, by changing the promoter and miRT sequences depending on the target cell population. Current limitations for the generalization of the approach is the restricted choice of miRT sequences and tissue-specific promoters due to the lack of cell-type specific miRNA expression profiles in adult or developing animals and poor characterization of transcriptional regulatory elements. Ongoing international projects should greatly improve the situation in the future^{15, 33, 34}. This LV gene transfer will facilitate *in vivo* silencing and offers new opportunities for local, cell-type specific, and regulated silencing. Thus, this tool will facilitate the study of gene candidates in various cellular pathways, reveal cell-autonomous functions, identify processes that depend on cell-

cell interactions in neurodegenerative diseases, and uncover the contribution of specific subpopulations of cells in pathological conditions.

MATERIALS AND METHODS

Plasmids

Constitutive silencing

The miR30-embedded shGFP (GeneArt, Invitrogen, Cergy-Pontoise, France)^{35, 36} was inserted into a SIN-PGK-GDNF-WPRE lentiviral plasmid containing the woodchuck post-regulatory element (WPRE) and encoding the Glial Cell line-Derived Neurotrophic factor (GDNF) under the control of the mouse phosphoglycerate promoter (PGK)¹³. The resulting plasmid SIN-PGK-miR30-shGFP was further modified to restrict transgene expression to astrocytes. For this, four fully homologous copies of the neuronal microRNA124 target sequence (miR124T) were added at the 3' end of the transgene (miRBase, Eurofins MWG Operon, Ebersberg, Germany)^{5, 28}. As a negative control, a lentiviral vector encoding the miR30-shUNIV sequence was used (pCCL-cPPT-PGK-miR30-shUNIV) (kindly provided by Prof. Naldini, Milano, Italy; sequence: GGTATCGATCACGA GACTAGC)³⁶.

Astrocyte-specific promoters and miRT detargeting strategies

The DsRednuc and mCherry reporter genes (Clontech, Saint-Germain-en-Laye, France) were used to assess LV tropism (SIN-promoter-DsRednuc-WPRE or SIN-promoter-mCherry-WPRE). The following promoters were used for astrocyte-specific expression: a 2 kb fragment of the human excitatory amino acid transporter 1 promoter (EAAT1; GeneArt, Invitrogen, Cergy-Pontoise, France; GenBank AF448436.1, nt: 1 to 2051)³⁷; the shortest form (681 bp) of the human glial fibrillary acidic protein (gfaABC₁D; courtesy of Dr. Brenner through the support of NIH grant NS39055, Birmingham, AL, USA; GenBank NG_008401.1, nt: 3292 to 3793 and 4916 to 5094);³⁸ and the 432 bp of the rat glutamine synthetase promoter (GS; GenBank M91651.1, nt: 2111 to 2543), which was amplified from rat genomic DNA with the following primers: 5'-CACCATCGATGGCTCGCTCAACAAAGGGTAA-3' and 5'-GGATCCCTCG GCTGTGGAGGGTTGCGG-3' (GenBank M91651.1, nt: 1 to 2132 with a CACC flanking sequence for oriented cloning, and nt: 2524 to 2543 for forward and reverse primers, respectively)²³. As a control, we used the 710 bp of the human cytomegalovirus

promoter (CMVa, Clontech, Saint-Germain-en-Laye, France; GenBank JQ302818.1, nt: 209 to 918).

Astrocyte-specific transgene expression was obtained by subcloning miR124T⁵, and miR9*T (miRBase, **AGAAACCAATAGATCGACATACTATTTCGAAAGAAACCAATAGATC GACAT**, GeneArt, Invitrogen, Regensburg, Germany) into LV transfer plasmids to obtain: SIN-CMVa-DsRednuc-WPRE-miR124T, SIN-EAAT1-DsRednuc-WPRE-miR124T, SIN-gfaABC₁D-DsRednuc-WPRE-miR124T, SIN-GS-DsRednuc-WPRE-miR124T, SIN-GS-mCherry-WPRE-miR124T, SIN-rGS-mCherry-WPRE-miR9*T and SIN-GS-mCherry-WPRE-miR9*T-miR124T.

Constitutive and tetracycline-regulated LV gene silencing

A cassette encoding the nuclear-localized green fluorescent protein (AcGFPnuc; Clontech, Saint-Germain-en-Laye, France) was inserted into the pCCL-MCS-cPPT-CMVb-tTA/S2-WPRE-TRE-SIN (kindly provided by Prof. Naldini, Milano, Italy)¹⁶. Two promoters were used to control tTA/S2 expression to generate vectors for astrocyte-specific silencing: CMVb (GenBank AY468486.1, nt: 2020 to 2624) or GS (GS; GenBank M91651.1, nt: 2111 to 2543) alone or in combination with four copies of the miR124T sequence. The final constructs were: pCCL-AcGFPnuc-cPPT-CMVb-tTA/S2-WPRE-TRE-SIN, pCCL-AcGFPnuc-cPPT-CMVb-tTA/S2-WPRE-miR124T-TRE-SIN and pCCL-AcGFPnuc-cPPT-GS-tTA/S2-WPRE-miR124T-TRE-SIN.

Silencing efficiency was determined with the pCCL-AcGFPnuc-cPPT-GS-tTA/S2-WPRE-miR124T-TRE-SIN, in which the AcGFPnuc was replaced with miR30-embedded shUNIV or shGFP. Silencing efficiency was compared with constitutive system by replacing the PGK promoter into the SIN-cPPT-PGK-miR30-shGFP with the rGS promoter (SIN-cPPT-rGS-miR30-shGFP).

The final Tet-regulated construct was constructed by inserting four copies of the miR9*T sequence were added upstream from the miR124T sequence to generate the final products: pCCL-miR30-shUNIV-cPPT-GS-tTA/S2-WPRE-miR9*T-miR124T-TRE-SIN and pCCL-miR30-shGFP-cPPT-GS-tTA/S2-WPRE-miR9*T-miR124T-TRE-SIN.

The specificity of the Tet-regulated construct was evaluated with the bicistronic vector expressing both GFP and mCherry (pCCL-mCherry-CMVmin-hPGK-eGFP-WPRE-SIN kindly provided by Prof Naldini, Milano, Italy; Brown et al, 2007).

LV expressing the reporter genes DsRed or blue fluorescent protein (DsRed and BFP, Clontech, Saint-Germain-en-Laye, France) under the control of the mouse PGK promoter (PGK; from -430 to +74 relative to the transcriptional start site (TSS); GenBank M18735.1 nt: 423 to 931) were used to facilitate the visualization of the infected area.

Lentiviral vector production

Lentiviral vectors were produced in Human Embryonic Kidney 293T cells (HEK 293T, mycoplasma negative, ATCC, LGC Standards GmbH, Germany), with the four-plasmid system, as described previously³⁹. The HIV-1 vectors were pseudotyped with either the vesicular stomatitis virus glycoprotein G (VSV-G) or the Mokola lyssavirus glycoprotein G (MOK-G)¹². Viruses were concentrated by ultracentrifugation and resuspended in phosphate-buffered saline (dPBS, Gibco, Life Technologies, Zug, Switzerland) with 1% bovine serum albumin (BSA, Sigma-Aldrich, Buchs, Switzerland). The viral particle content of each batch was determined by p24 antigen enzyme-linked immunosorbent assay (p24 ELISA, RETROtek; Kampenhout, Belgium). The stocks were finally stored at -80°C until use.

Animals

Adult males and females BAC-GLT1-eGFP, BAC-GLAST-DsRed (courtesy of Prof. J. Rothstein, Baltimore, MD, USA)¹⁴, Tg(Drd2-EGFP)S118Gsat/Mmnc (BAC-Drd2-eGFP, Mutant Mouse Regional Resource Center, USA)¹ and C57Bl/6 (Charles River, France) between 3 and 10 months old were used for *in vivo* experiments. The animals were housed in a temperature-controlled room (22°C±1°C) and maintained on a 12 h light/night cycle. Food and water were available *ad libitum*. All experimental procedures were performed in strict accordance with the recommendations of the European Community directive (86/609/EEC) and Swiss legislation about the care and use of laboratory animals. All experiments involving animals were performed once. Sample size was chosen to take into

account statistical variability due to surgical procedure based on previous studies ³⁶. No randomization was used to determine group inclusion and experiments were not performed in blind.

Stereotaxic procedure

Concentrated viral stocks were thawed on ice and resuspended by repeated pipetting. Low doses of LV were used (100 and 200 ng p24 in PBS/1% BSA) to facilitate the analysis of the tropism and avoid saturation of transcriptional activities. For co-transduction with viral vectors expressing fluorescent proteins, between 50 and 100 ng of LV-DsRed/BFP were added to the viral vector of interest.

Mice were anesthetized by intraperitoneal injection of a mixture of 100 mg/kg ketamine (Ketasol, Graeb, Bern, Switzerland) and 10 mg/kg xylazine (Rompun, Bayer Health Care, Uznach, Switzerland). Suspensions of lentiviral vectors were injected into the mouse striatum with a 34-gauge blunt-tip needle linked to a Hamilton syringe by a polyethylene catheter. Stereotaxic coordinates were: anteroposterior +1 mm from bregma; mediolateral +/-1.8 mm and dorsoventral -3.5 mm from the skull, with the tooth bar set at -3.3 mm. Mice received a total volume of 3 µl of the vector preparation, administered at a rate of 0.2 µl/min. At the end of injections, needles were left in place for 5 min before being slowly removed. The skin was sutured with 6-0 Prolene suture (B-Braun Mediacal SA, Sempach, Switzerland) and mice were allowed to recover on a heating mat. Number of animals (biological replicates) used in each experiments is indicated in the Figure legends. The only exclusion criterion was a problem encountered during the injection procedure.

Brain processing

Two or three weeks post-lentiviral injection, the animals were killed by an overdose of sodium pentobarbital (NaCl, B-Braun, Sempach, Germany; Esconarkon, Streuli, Uznach, Germany) and transcardially perfused with a 4% paraformaldehyde solution (4% PFA; Electron Microscopy Sciences, Hatfield). The brains were removed and post-fixed in 4% PFA for 12 h and then cryoprotected in 20% sucrose / PBS for 3 h and in 30% sucrose / PBS for

24 h. A sledge microtome with a freezing stage at -30 °C (Leica SM2010R, Biosystems Switzerland, Nunningen, Switzerland) was used to cut coronal sections between 20 and 30 µm thickness. Slices throughout the entire striatum were collected and stored in tubes as free-floating sections in anti-freeze solution (18% sucrose, 0.25% sodium azide, ethylene glycol and sodium phosphate 50mM, pH = 7.4). Slices were then stored at -20°C.

Immunohistochemistry

The following primary antibodies were used: mouse monoclonal anti-neuronal nuclei antibody (NeuN, 1/200; MAB377, Millipore, Molsheim, France); rabbit polyclonal anti-neuronal nuclei antibody (NeuN, 1/1000, ABN78, Millipore, Zug, Switzerland) and goat polyclonal anti-mCherry antibody (mCherry, 1/1000, AB0040-200, SicGen, Lisboa, Portugal). For antibodies produced in mice, immunostaining was performed with the mouse-on-mouse detection kit (Vectashield M.O.M kit, Vector Lab Inc, Clinisciences, Nanterre, France). For other antibodies, free floating slices were rinsed 3 x 10 minutes in PBS (Laboratorium Dr Bichsel AG, Interlaken, Switzerland), followed by the saturation of non-specific sites in PBS containing 10% BSA (Sigma-Aldrich, Buchs, Switzerland) and 0.1% Tritton X100 (Fluka, Sigma-Aldrich, Buchs, Switzerland) for 1h at room temperature under agitation. Primary antibodies were incubated overnight at 4°C under agitation. Slices were rinsed 3 x 10 minutes in PBS and incubated with the secondary antibodies for 1h at room temperature under agitation. The following secondary antibodies were used: anti-mouse IgG AlexaFluor 350 (1/500, A10035, Life Technologies, Saint Aubin, France), donkey anti-goat IgG AlexaFluor 568 (1/1000, A11057, Invitrogen, Life Technologies, Zug, Switzerland). Slices were then rinsed 3 x 10 minutes in PBS, followed by mounting with Vectashield mounting medium for fluorescence with DAPI (Vector Lab Inc, Burlingame, CA, USA).

Image acquisition and quantitative analysis

For co-localization studies, images of the sections labeled for GLT1-eGFP and NeuN were acquired with a 40x objective on a Leica DM6000B microscope (Leica, Nanterre, France) equipped with an automated motorized stage and image acquisition software (MorphoStrider, Explora nova, La Rochelle, France). The number of DsRed2nuc-NeuN-

positive cells and DsRed2nuc-GLT1-eGFP-positive cells were quantified by ImageJ software (<http://rsb.info.nih.gov/ij/>, NIH, Bethesda, MD, USA) to determine the percentage of astrocytes or neurons expressing the transgene.

For the GFP silencing studies, mosaic images were acquired with an Olympus BX 40 microscope at a 10x objective (Olympus, Le Mont-sur-Lausanne, Switzerland), with Morphostrider software (Explora Nova, La Rochelle, France). The area of GFP loss was measured with Mercator Pro software (Explora Nova, La Rochelle, France) along the entire infected area to determine the volume of GFP silencing. Mosaic images for silencing efficiency comparisons between constitutive and Tet-regulated systems were acquired with the Zeiss AxioVision at 10x (Zeiss, Carl Zeiss Microscopy GmbH, Göttingen, Germany). Mosaic images for the evaluation of silencing efficiency of the MOK/LV-shGFP-miR9*^T-miR124^T were acquired with the Zeiss AxioScan Z1 (Zen software, Zeiss, Carl Zeiss Microscopy GmbH, Göttingen, Germany).

Mean fluorescence intensity quantifications for the silencing efficiency comparison between Tet-regulated and constitutive system were done based on acquisitions performed with a 40x oil immersion objective with an inverted confocal microscope Zeiss LSM 510 META (LSM software, Carl Zeiss Microscopy GmbH, Göttingen, Germany). Regions at the periphery of the transduced area were delineated with ImageJ software and the mean fluorescence intensity normalized on the area of the region was determined for each groups.

For the quantification of the bicistronic vector, images were acquired with a 63x oil immersion objective with an inverted confocal microscope Zeiss LSM 510 META (LSM software, Carl Zeiss Microscopy GmbH, Göttingen, Germany). The mCherry fluorescence intensity is used as a reference to determine the GFP expression level (measurement of mCherry/GFP fluorescence ratio). Acquisition parameters of the Zeiss LSM 510 META and of the camera were maintained constant for all the groups. Neurons expressing both GFP and mCherry were delimited and the mean fluorescence intensity of each channel was measured with the ImageJ software.

Statistical analysis

Data are presented as the mean \pm standard error of the mean (SEM). Statistical analysis was carried out with Statistica software (Statsoft, Maisons-Alfort, France) and the threshold of significance was maintained at $p < 0.05$, without correction for multiple comparisons. All statistical analysis are two-sided tests.

Statistical analyses to compare two independent groups were done with paired or unpaired Student *t* test. When more than two groups were compared, one-way ANOVA with a Newman-Keuls post-hoc was used. A one-way ANOVA with a Newman-Keuls post-hoc was performed on Arcsine transformed data to analyze the percentages of infected neurons and astrocytes. Normality of the data and equality of variances between groups was assessed as a prerequisite to perform statistical analysis.

ACKNOWLEDGEMENTS

This work was partially supported by the CEA and the European Community's Seventh Framework Program FP7/2007–2013 under the grant agreement n° HEALTH-F5-2008-222925 (NEUGENE) and by the Swiss National Science Foundation 31003A-140945. We want to thank Carole Malgorn (CEA, France) and Lydie Boussicault (CEA, France) for their help in genotyping mice, Fanny Petit (CEA, France), Martine Guillermier (CEA, France), Diane Houitte (CEA, France), Virginie Zimmer (LCMN, Lausanne) and Alexia Spoerl (LCMN, Lausanne) for help with animal experiments, Dr Emmanuel Brouillet (CEA, France) and the Cellular Imaging Facility (CIF, Lausanne) for their advice about microscopic acquisitions.

Conflict of interest

The authors of the present manuscript have no competing financial interests.

Supplementary information are available at the *Gene Therapy's* website.

REFERENCES

1. Gong S, Zheng C, Doughty ML, Losos K, Didkovsky N, Schambra UB *et al.* A gene expression atlas of the central nervous system based on bacterial artificial chromosomes. *Nature* 2003; **425**(6961): 917-25.
2. Pfrieder FW, Slezak M. Genetic approaches to study glial cells in the rodent brain. *Glia* 2012; **60**(5): 681-701.
3. Kay MA, Glorioso JC, Naldini L. Viral vectors for gene therapy: the art of turning infectious agents into vehicles of therapeutics. *Nat Med* 2001; **7**(1): 33-40.
4. Kirik D, Bjorklund A. Modeling CNS neurodegeneration by overexpressing disease causing proteins using viral vectors. *TINS* 2003; **26**: 386-392.
5. Delzor A, Escartin C, Deglon N. Lentiviral vectors: a powerful tool to target astrocytes in vivo. *Curr Drug Targets* 2013; **14**(11): 1336-46.
6. Merienne N, Le Douce J, Faivre E, Deglon N, Bonvento G. Efficient gene delivery and selective transduction of astrocytes in the mammalian brain using viral vectors. *Front Cell Neurosci* 2013; **7**: 106.
7. Naldini L, Blomer U, Gallay P, Ory D, Mulligan R, Gage FH *et al.* In vivo gene delivery and stable transduction of nondividing cells by a lentiviral vector. *Science* 1996; **272**(5259): 263-7.
8. Watson DJ, Kobinger GP, Passini MA, Wilson JM, Wolfe JH. Targeted transduction patterns in the mouse brain by lentivirus vectors pseudotyped with VSV, Ebola, Mokola, LCMV, or MuLV envelope proteins. *Mol Ther* 2002; **5**(5 Pt 1): 528-37.

9. Liu B, Paton JF, Kasparov S. Viral vectors based on bidirectional cell-specific mammalian promoters and transcriptional amplification strategy for use in vitro and in vivo. *BMC Biotechnol* 2008; **8**: 49.
10. Drinkut A, Tereshchenko Y, Schulz JB, Bahr M, Kugler S. Efficient gene therapy for Parkinson's disease using astrocytes as hosts for localized neurotrophic factor delivery. *Mol Ther* 2012; **20**(3): 534-43.
11. Brown BD, Venneri MA, Zingale A, Sergi Sergi L, Naldini L. Endogenous microRNA regulation suppresses transgene expression in hematopoietic lineages and enables stable gene transfer. *Nat Med* 2006; **12**(5): 585-91.
12. Colin A, Faideau M, Dufour N, Auregan G, Hassig R, Andrieu T *et al.* Engineered lentiviral vector targeting astrocytes in vivo. *Glia* 2009; **57**(6): 667-79.
13. Deglon N, Tseng JL, Bensadoun JC, Zurn AD, Arsenijevic Y, Pereira de Almeida L *et al.* Self-inactivating lentiviral vectors with enhanced transgene expression as potential gene transfer system in Parkinson's disease. *Hum Gene Ther* 2000; **11**(1): 179-90.
14. Regan MR, Huang YH, Kim YS, Dykes-Hoberg MI, Jin L, Watkins AM *et al.* Variations in promoter activity reveal a differential expression and physiology of glutamate transporters by glia in the developing and mature CNS. *J Neurosci* 2007; **27**(25): 6607-19.
15. Hawrylycz MJ, Lein ES, Guillozet-Bongaarts AL, Shen EH, Ng L, Miller JA *et al.* An anatomically comprehensive atlas of the adult human brain transcriptome. *Nature* 2012; **489**(7416): 391-9.

16. Vigna E, Amendola M, Benedicenti F, Simmons AD, Follenzi A, Naldini L. Efficient Tet-dependent expression of human factor IX in vivo by a new self-regulating lentiviral vector. *Mol Ther* 2005; **11**(5): 763-75.
17. Brown BD, Gentner B, Cantore A, Colleoni S, Amendola M, Zingale A *et al.* Endogenous microRNA can be broadly exploited to regulate transgene expression according to tissue, lineage and differentiation state. *Nat Biotechnol* 2007; **25**(12): 1457-67.
18. Liu B, Xu H, Paton JF, Kasparov S. Cell- and region-specific miR30-based gene knock-down with temporal control in the rat brain. *BMC Mol Biol* 2010; **11**: 93.
19. Aschauer DF, Kreuz S, Rumpel S. Analysis of transduction efficiency, tropism and axonal transport of AAV serotypes 1, 2, 5, 6, 8 and 9 in the mouse brain. *PLoS One* 2013; **8**(9): e76310.
20. Pertusa M, Garcia-Matas S, Mammeri H, Adell A, Rodrigo T, Mallet J *et al.* Expression of GDNF transgene in astrocytes improves cognitive deficits in aged rats. *Neurobiol Aging* 2008; **29**(9): 1366-79.
21. Jakobsson J, Ericson C, Jansson M, Bjork E, Lundberg C. Targeted transgene expression in rat brain using lentiviral vectors. *J Neurosci Res* 2003; **73**(6): 876-85.
22. Yaguchi M, Ohashi Y, Tsubota T, Sato A, Koyano KW, Wang N *et al.* Characterization of the properties of seven promoters in the motor cortex of rats and monkeys after lentiviral vector-mediated gene transfer. *Hum Gene Ther Methods* 2013; **24**(6): 333-44.

23. Mearow KM, Mill JF, Vitkovic L. The ontogeny and localization of glutamine synthetase gene expression in rat brain. *Brain Res Mol Brain Res* 1989; **6**(4): 223-32.
24. Brenner M, Messing A. GFAP Transgenic Mice. *Methods* 1996; **10**(3): 351-64.
25. Vigna E, Cavalieri S, Ailles L, Geuna M, Loew R, Bujard H *et al.* Robust and efficient regulation of transgene expression in vivo by improved tetracycline-dependent lentiviral vectors. *Mol Ther* 2002; **5**(3): 252-61.
26. Régulier E, Pereira de Almeida L, Sommer B, Aebischer P, Déglon N. Dose-dependent neuroprotective effect of CNTF delivered via tetracycline-regulated lentiviral vectors in the quinolinic acid rat model of Huntington's disease. *Hum Gene Ther* 2002; **13**(15): 1981-1990.
27. Blesch A, Conner J, Pfeifer A, Gasmi M, Ramirez A, Britton W *et al.* Regulated lentiviral NGF gene transfer controls rescue of medial septal cholinergic neurons. *Mol Ther* 2005; **11**(6): 916-25.
28. Brown BD, Cantore A, Annoni A, Sergi LS, Lombardo A, Della Valle P *et al.* A microRNA-regulated lentiviral vector mediates stable correction of hemophilia B mice. *Blood* 2007; **110**(13): 4144-52.
29. Ko MH, Kim S, Hwang do W, Ko HY, Kim YH, Lee DS. Bioimaging of the unbalanced expression of microRNA9 and microRNA9* during the neuronal differentiation of P19 cells. *FEBS J* 2008; **275**(10): 2605-16.
30. Cheng LC, Pastrana E, Tavazoie M, Doetsch F. miR-124 regulates adult neurogenesis in the subventricular zone stem cell niche. *Nat Neurosci* 2009; **12**(4): 399-408.

31. Gentner B, Naldini L. Exploiting microRNA regulation for genetic engineering. *Tissue Antigens* 2012; **80**(5): 393-403.
32. Hutvagner G, Zamore PD. A microRNA in a multiple-turnover RNAi enzyme complex. *Science* 2002; **297**(5589): 2056-60.
33. Portales-Casamar E, Swanson DJ, Liu L, de Leeuw CN, Banks KG, Ho Sui SJ *et al.* A regulatory toolbox of MiniPromoters to drive selective expression in the brain. *Proc Natl Acad Sci U S A* 2010; **107**(38): 16589-94.
34. Consortium EP, Bernstein BE, Birney E, Dunham I, Green ED, Gunter C *et al.* An integrated encyclopedia of DNA elements in the human genome. *Nature* 2012; **489**(7414): 57-74.
35. Shin KJ, Wall EA, Zavzavadjian JR, Santat LA, Liu J, Hwang JI *et al.* A single lentiviral vector platform for microRNA-based conditional RNA interference and coordinated transgene expression. *Proc Natl Acad Sci U S A* 2006; **103**(37): 13759-64.
36. Drouet V, Perrin V, Hassig R, Dufour N, Auregan G, Alves S *et al.* Sustained effects of nonallele-specific Huntingtin silencing. *Ann Neurol* 2009; **65**(3): 276-85.
37. Kim S-Y, Choi S-Y, Chao W, Volsky DJ. Transcriptional regulation of human excitatory amino acid transporter 1 (EAAT1): cloning of the EAAT1 promoter and characterization of its basal and inducible activity in human astrocytes. *Journal of Neurochemistry* 2003; **87**(6): 1485-1498.

38. Lee Y, Messing A, Su M, Brenner M. GFAP promoter elements required for region-specific and astrocyte-specific expression. *Glia* 2008; **56**(5): 481-93.

39. Hottinger AF, Azzouz M, Deglon N, Aebischer P, Zurn AD. Complete and long-term rescue of lesioned adult motoneurons by lentiviral-mediated expression of glial cell line-derived neurotrophic factor in the facial nucleus. *J Neurosci* 2000; **20**(15): 5587-93.

FIGURE LEGENDS

Figure 1: A miRNA detargeting approach is not suitable for LV constitutively expressed shRNA

(a): VSV/LV-shUNIV (n = 4), VSV/LV-shGFP-miR124T (n= 4) and VSV/LV-shGFP (n = 4) were co-injected with VSV/LV-DsRed into the striatum of BAC Drd2-eGFP transgenic mice to evaluate the hypothesis that the miR124T is cleaved from the shRNA. Confocal pictures show GFP loss in LV-shGFP-miR124T and LV-shGFP groups surrounded by DsRed fluorescence, revealing that GFP loss is not due to neuronal death following LV injection. Scale bar = 50µm

(b): Silencing efficiency was quantified based on the volume of GFP fluorescence. One-way ANOVA and Newman-Keuls post-hoc analysis reveals efficient GFP silencing in both LV-shGFP and LV-shGFP-miR124T but no differences between LV-shGFP and LV-shGFP-miR124T. * $p < 0.05$, results are presented as mean \pm SEM.

(c): Schematic representation of the hypothesis of miR124T cleavage. LVs enter both neurons and astrocytes, with a preferential tropism for astrocytes depending on the envelope. Transcription of the miR30-embedded shGFP and natural processing releases the 20 bp shGFP without the miR124T sequences, which impairs detargeting in neurons and results in GFP silencing in both cell populations.

(d): Schematic representation of the alternative strategy based on the Tet-regulated LV. LV expressing the Tet-regulated system enters neurons and astrocytes. In astrocytes, the expressed tTA/S2 dimerizes and recognizes the TRE to induce shGFP expression, leading to GFP silencing. In neurons, the residual transcription of the astrocytic promoter generates a tTA/S2 mRNA containing the miRT sequences. Hybridization of the endogenous neuronal miRNA degrades the tTA/S2 mRNA, which results in the loss of shGFP expression in neurons.

Figure 2: Effect of astrocytic promoters and miR124T sequences on LV tropism

(a) and (c): Microscope acquisition of BAC GLT1-eGFP transgenic mice infected with LV expressing DsRednuc under the CMVa, EAAT1, gfaABC₁D or GS promoter alone (a) or in combination with four copies of the miR124T (c). Acquisition parameters were not maintained constant between the groups because of differences in strength of promoter activity. Scale bar = 10µm

(b): Colocalization between DsRednuc and eGFP positive-astrocytes or NeuN-positive neurons for the CMVa (n = 5), EAAT1 (n = 5), gfaABC₁D (n = 6) and GS (n = 6) groups. One-way ANOVA on arcsine-transformed values for all the groups and Newman-Keuls post-hoc analysis reveals statistical differences only between CMVa and GS groups. * $p < 0.05$, results are presented as mean \pm SEM.

(d): Percentage of DsRednuc positive-cells colocalizing with NeuN or eGFP in the CMVa-miR124T (n = 4), EAAT1-miR124T (n = 5), gfaABC₁D-miR124T (n = 6) and GS-miR124T (n = 6) groups. One-way ANOVA reveals no statistical differences between the groups, results are presented as mean \pm SEM.

Figure 3: Efficiency and specificity of the Tet-regulated LV expressing shRNA

(a): Schematic representation of the GS-shGFP (left) and Tet-shGFP (right) constructs.

(b): Mosaic acquisitions of the infected area for the GS-shGFP (left), Tet-shGFP (middle) and a non-injected groups (right). Pictures show an extended loss of GFP signal in both constitutive and Tet-regulated system with no major differences between the two groups.

(c): Quantification of the fluorescence intensity of the infected area in GS-shGFP (n = 3) and Tet-shGFP (n = 3). Confocal acquisitions were performed at the periphery of the infected area to determine the differential silencing efficiency between the two groups. Mean GFP fluorescence intensity shows that the GFP silencing is more efficient with the Tet-regulated system than with the constitutive construct. Paired Student t test, ** $p < 0.01$, results are presented as mean \pm SEM.

(d): Schematic representation of the bicistronic vector expressing both GFP and mCherry in neurons under the PGK or CMVmin promoters. High magnification pictures were acquired at

constant acquisition parameters. The mean fluorescence intensity per cell was calculated for shGFP-miR124T (n = 4) and shUNIV-miR124T (n = 5) groups 2 weeks post-transduction. Unpaired Student *t*-test reveals that the GFP/mCherry ratio in the shGFP-miR124T group is significantly lower (11%) than that of the shUNIV-miR124T group, revealing residual GFP silencing in neurons. Data are represented as mean \pm SEM. * $p < 0.05$

Figure 4: Efficient, astrocyte-specific gene silencing by the combinatorial effect of miR9*T-miR124T detargeting

(a): Schematic representation of the final Tet-regulated LV for astrocyte-specific gene silencing. In this version of the vector, tTA/S2 expression is regulated by the GS promoter and four copies of both miR9*T and miR124T sequences.

(b): Brains were processed three weeks post-transduction and the GFP silencing volume was quantified. Slice scanning and confocal acquisitions show extensive GFP loss in the hemisphere treated with the Tet-shGFP-miR9*T-miR124T but not in the control Tet-shUNIV-miR9*T-miR124T. Scale bar = 50 μ m

(c): Paired Student *t*-test reveals that the volume of GFP silencing in the Tet-shGFP-miR9*T-miR124T (n = 7) is significantly higher than in the Tet-shUNIV-miR9*T-miR124T (n = 7) group. Results are presented as mean \pm SEM, *** $p < 0.001$.

(d): Neurons were infected with the Tet-shUNIV-miR9*T-miR124T (n = 8), Tet-shGFP-miR9*T-miR124T (n = 10) or PGK-shGFP (n = 10) vector in combination with the bicistronic vector expressing both GFP and mCherry to assess astrocytic specificity of the viral construct. High magnification confocal pictures at constant acquisition parameters were performed to quantify the mean fluorescence intensity per cell. Scale bar = 20 μ m

(e): One-way ANOVA and Newman-Keuls post-hoc analysis reveal that the GFP/mCherry ratio of both Tet-shUNIV-miR9*T-miR124T and Tet-shGFP-miR9*T-miR124T groups are significantly different from that of the PGK-shGFP group. There was no significant difference between Tet-shUNIV-miR9*T-miR124T and Tet-shGFP-miR9*T-miR124T groups, suggesting that residual GFP silencing does not occur in neurons in the Tet-shGFP-miR9*T-miR124T group. Results are presented as mean \pm SEM, ** $p < 0.01$.

SUPPLEMENTARY INFORMATIONS

Supplementary Figure 1: Differential expression of *gfap* and *glul* in the mouse striatum

(a): Tridimensional visualization of the *gfap* and *glul* (GS) expression in MRI coordinate space from Allen Brain Atlas (Allen Institute for Brain Science, Seattle (WA), Available from: <http://www.brain-map.org>, reconstructed with Brain Explorer 2 software, available from: <http://human.brain-map.org/static/brainexplorer>),¹⁵. Expression levels from in-situ hybridization for *gfap* (up, red dots) and *glul* (bottom, cyan dots) were aligned on mouse MRI data on the coronal and sagittal plans. Dots size and density suggest a stronger expression of *glul* compared with *gfap*.

(b): Microarray expression data from striatum samples for *gfap* and *glul* taken from the Allen Brain Atlas reveals a strong differences of expression between *gfap* and *glul* in the mouse striatum. Scale is log2 transformed, results are presented as mean \pm SEM.

Supplementary Figure 2: Functionality and tropism of the Tet-regulated LV

(a): Schematic representation of the Tet-regulated LV expressing AcGFPnuc. For this experiment, the GS promoter and four copies of the miR124T sequence regulate the tTA/S2. AcGFPnuc expression is driven from the TRE.

(b): Brains were processed three weeks post-transduction and colocalization between AcGFPnuc and DsRed-positive astrocytes or NeuN-positive neurons was quantified for the CMVb, CMVb-miR124T and GS-miR124T groups (n = 4 for all groups). One-way ANOVA reveals no statistical differences between the groups. Results are presented as mean \pm SEM.

Supplementary Figure 3: Efficient neuronal detargeting with a miR9*^T sequence

(a): The detargeting efficiency of miR124T and miR9*^T sequences was compared with LV expressing mCherry in a constitutive system. High magnification confocal acquisitions of the mCherry-positive area were performed for the analysis. Scale bar = 20µm

(b): Quantification of the number of mCherry-positive cells colocalizing with the eGFP-positive astrocytes. Percentages were transformed with the arcsine transformation to perform statistical analysis. Unpaired Student *t*-test reveals no statistical differences between the MOK/LV-GS-mCherry-miR124T (GS-miR124T, n = 6) and MOK/LV-GS-mCherry-miR9*^T (GS-miR9*^T, n = 4) groups, suggesting that miR9*^T sequences can be used for neuronal miRT detargeting. Results are presented as mean ± SEM.

Figure 1

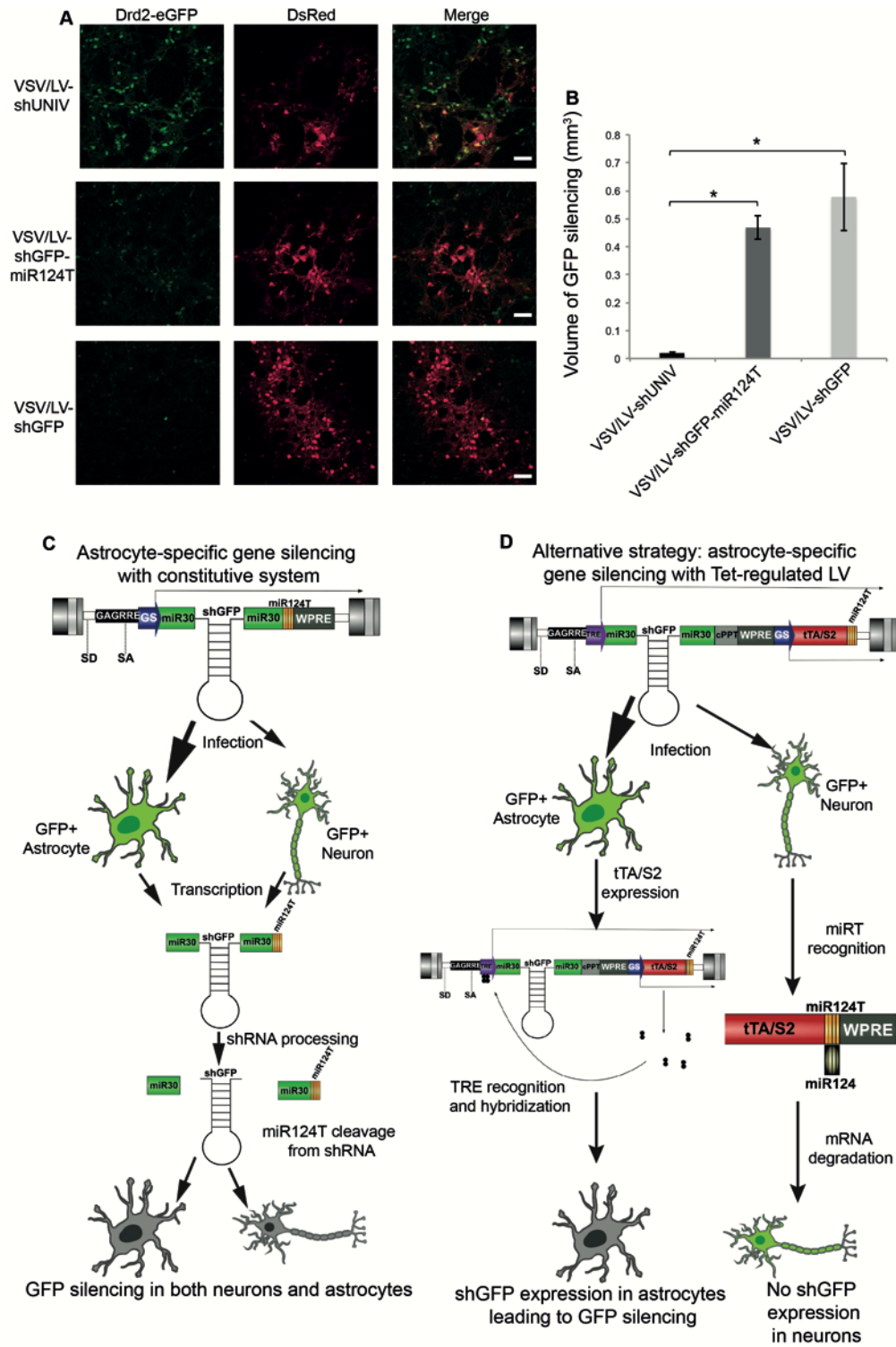


Figure 2

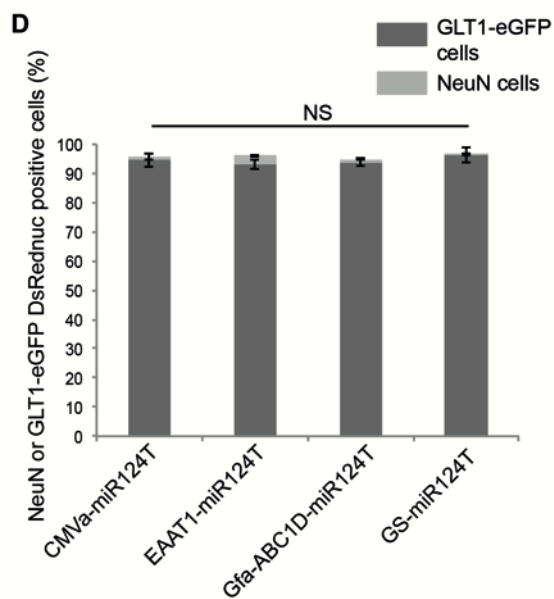
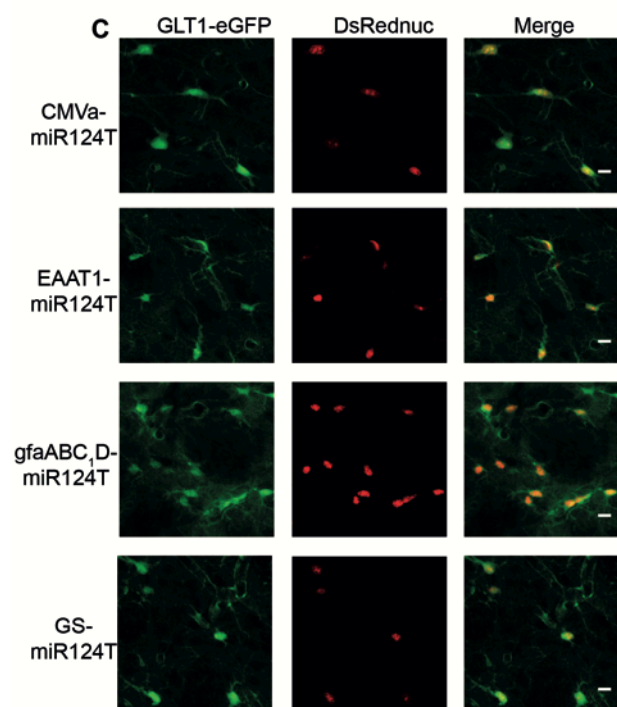
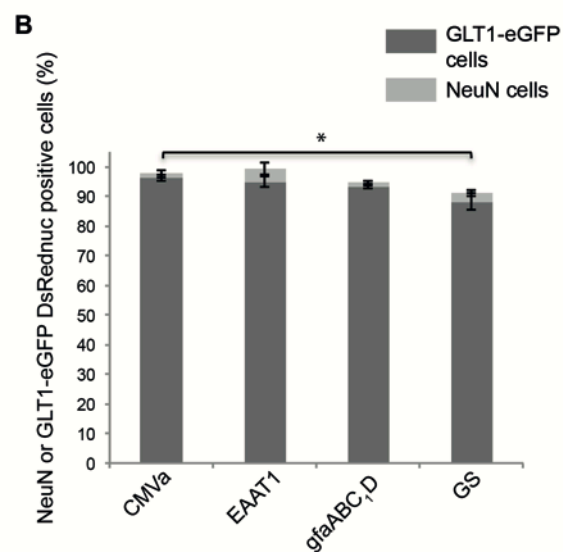
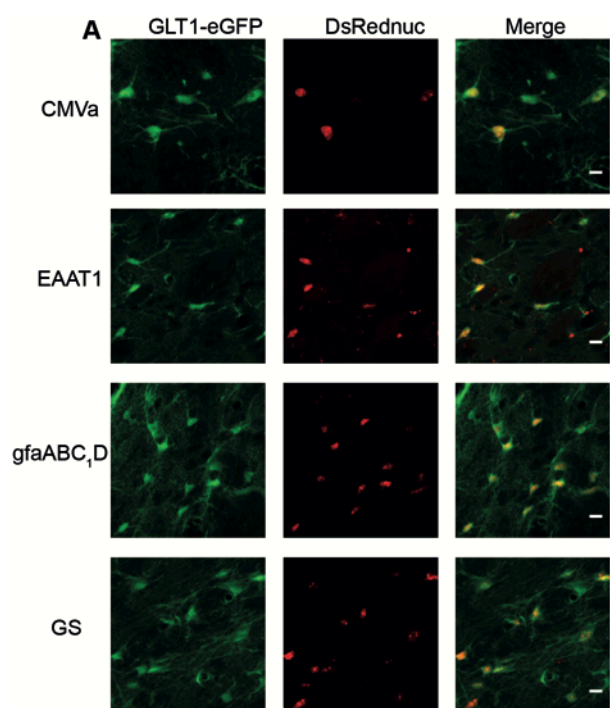


Figure 3

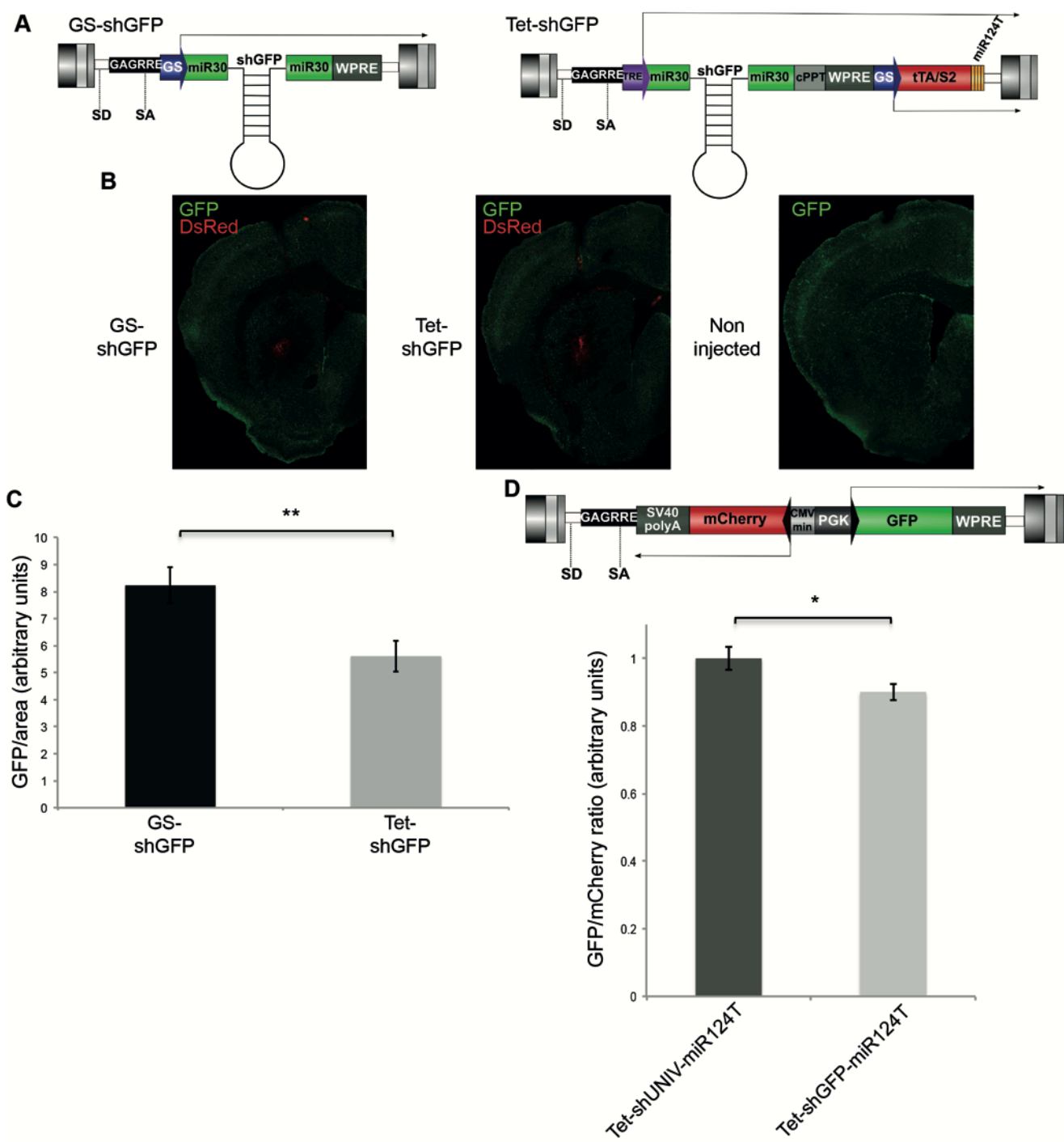


Figure 4

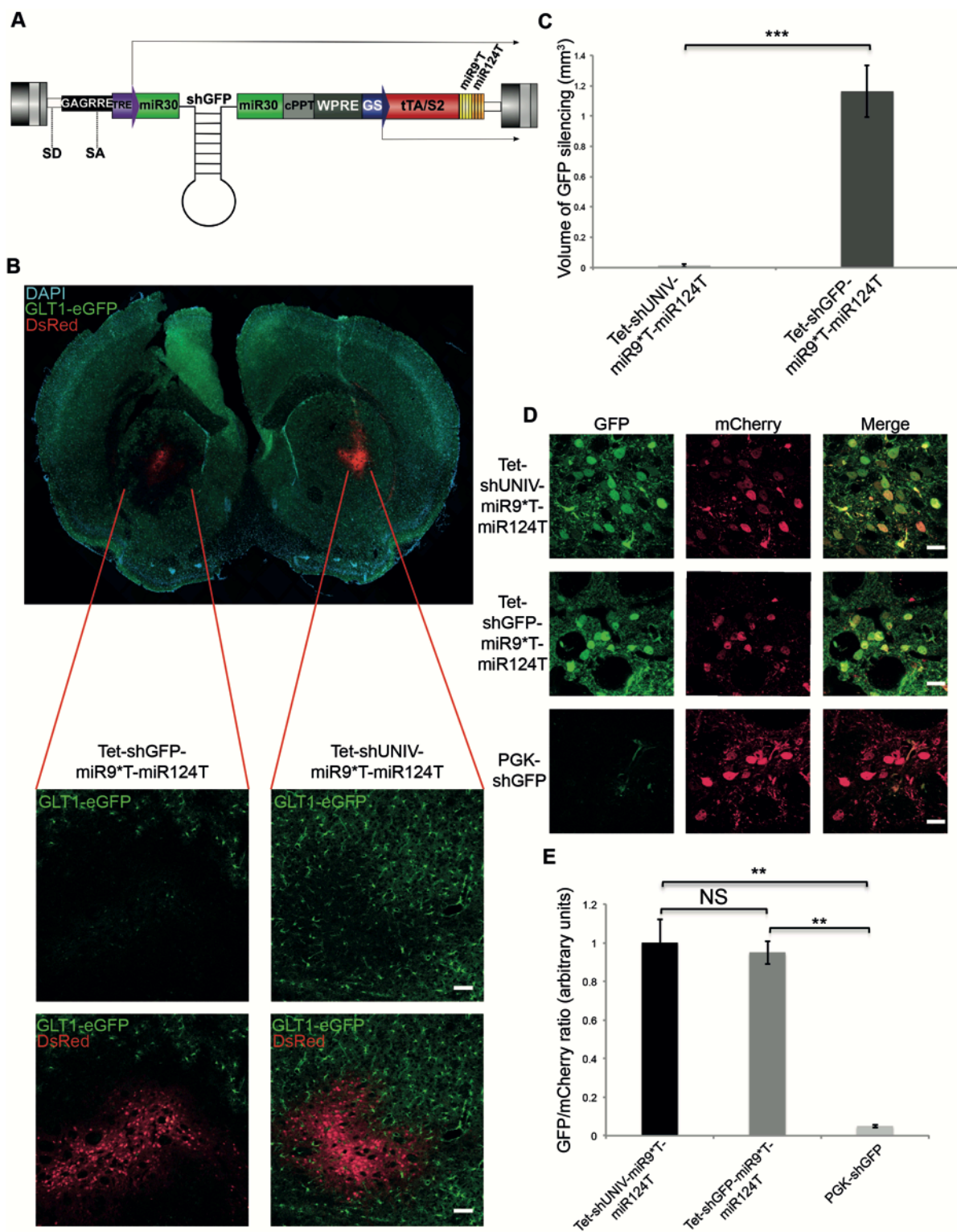


Figure S1

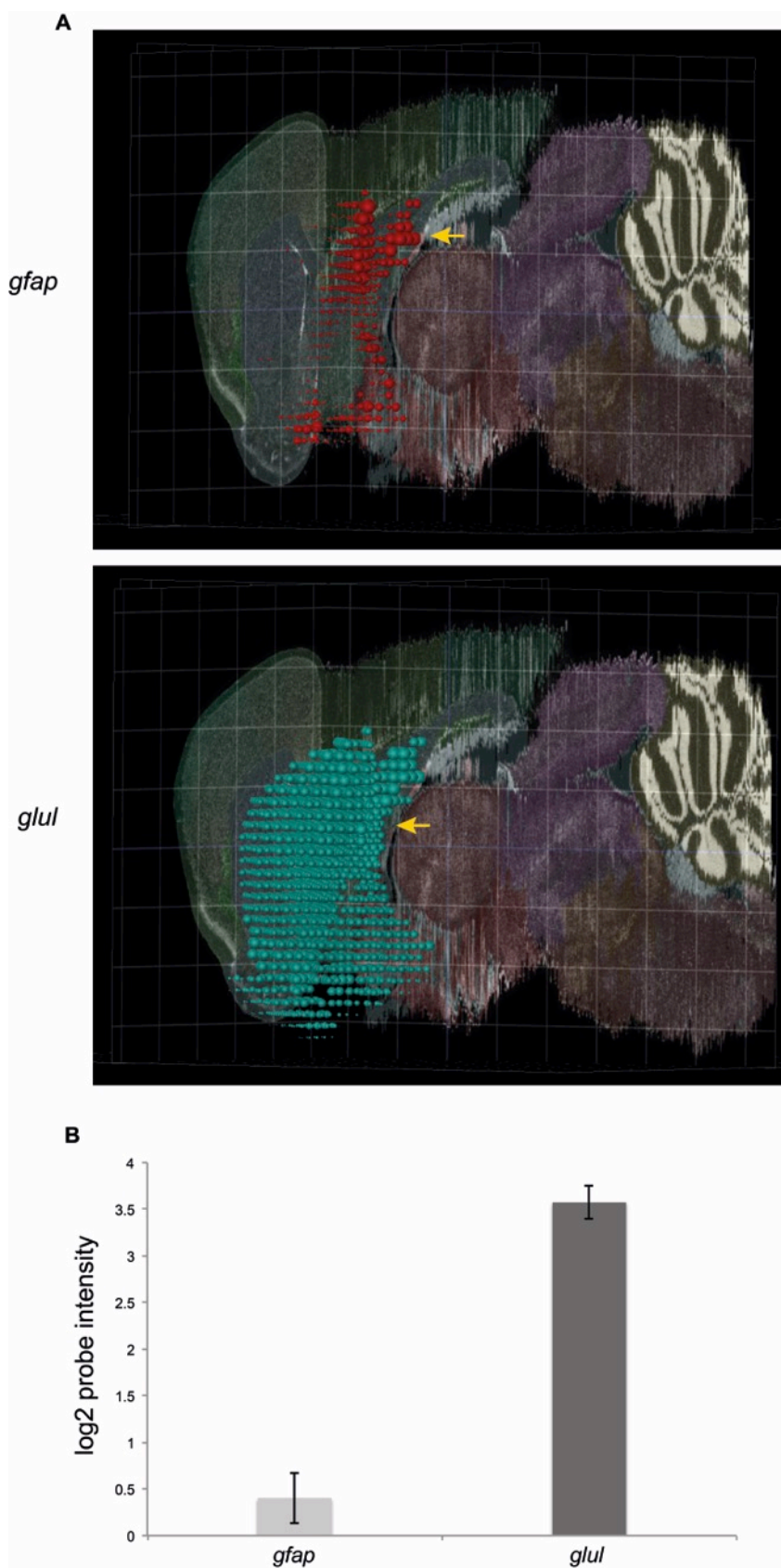
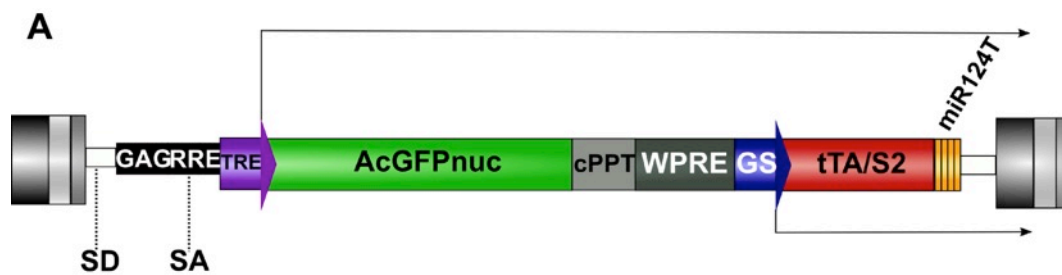


Figure S2



B

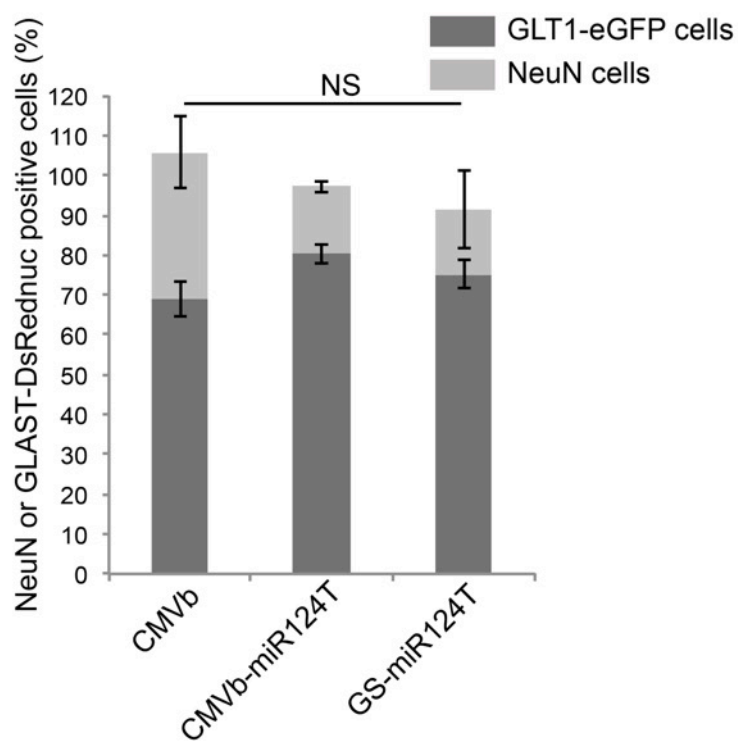
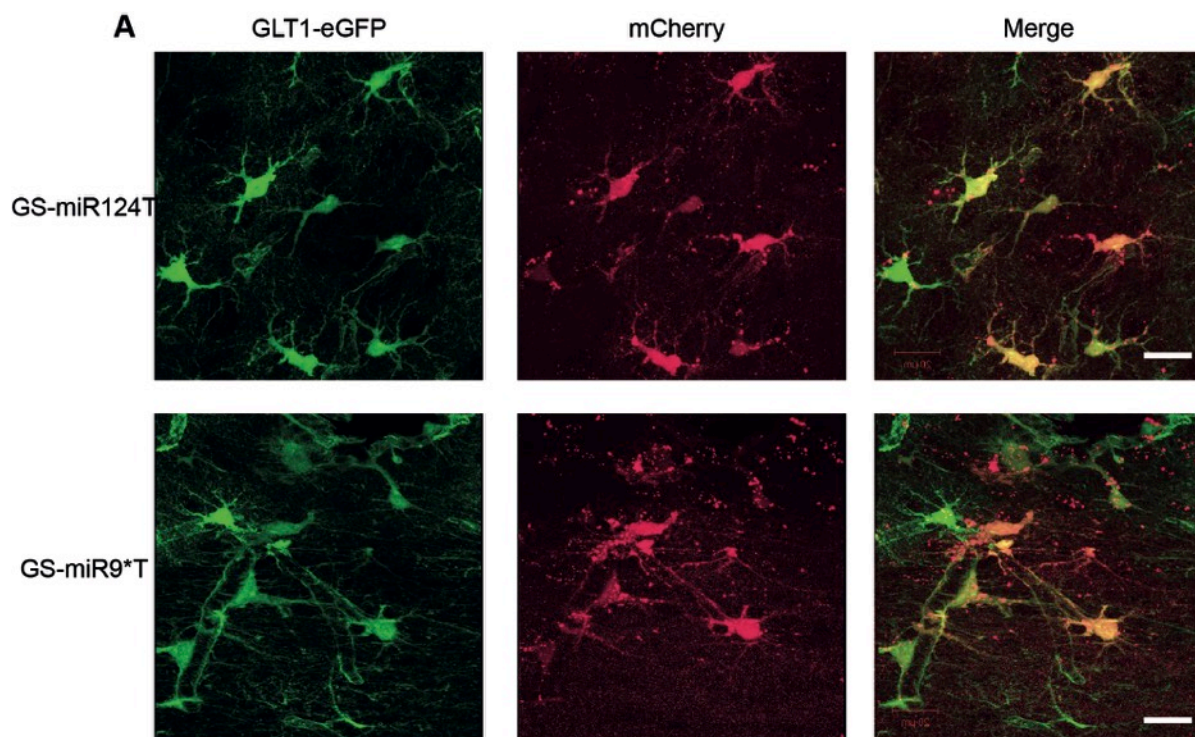


Figure S3



B

